Repurposing naproxen as a potential antiviral agent against SARS-CoV-2

Milad Lagzian
Department of Biology, Faculty of Science, University of Sistan and Baluchestan
Reza Valadan
Department of Immunology, Faculty of Medicine and Molecular and Cell Biology Research Center, Mazandaran University of Medical Sciences
Majid Saeedi
Department of Pharmaceutics, Faculty of Pharmacy and Pharmaceutical Sciences Research Center, Mazandaran University of Medical Sciences
Fatemeh Roozbeh
Infectious specialist, Mazandaran University of Medical Sciences
Akbar Hedayatizadeh-Omran
Gastrointestinal Cancer Research Center, Mazandaran University of Medical Sciences
Massoud Amanlou
Department of Medicinal Chemistry, Faculty of Pharmacy, Tehran University of Medical Sciences
Reza Alizadeh-Navaei (reza_nava@yahoo.com)
Gastrointestinal Cancer Research Center, Mazandaran University of Medical Sciences

Research Article

Keywords: Repurposing, Naproxen, molecular docking, molecular dynamics, SARS-CoV-2. nucleocapsid

Posted Date: April 7th, 2020

DOI: https://doi.org/10.21203/rs.3.rs-21833/v1

Abstract

The Outbreak of severe acute respiratory syndrome coronavirus 2 (SARS-CoV-2) infections in late 2019 in China and many other countries around the world necessitate immediate action to develop new drugs against the virus. Repurposing of existing drugs for new targets is a fast, safe and unexpansive approach for this goal. Studies have shown that naproxen could specifically interact with the RNA binding domain of nueclporteins of RNA viruses such as the influenza virus. Therefore, this study aimed to evaluate the binding properties of naproxen to the nucleocapsid protein of SARS-CoV-2. 3D structure of N and C terminal domains of SARS-CoV- 2 nucleocapsid were constructed and each were docked with naproxen and analyzed during 100 ns of molecular dynamics. The results showed that naproxen interacts with the N terminal domain of the nucleocapsid via two salt bridges with Arg 88 and 92 and a network of h-bonds. Molecular dynamics analysis was also revealed that all the coordinations of naproxen with N terminal domain were kept during 100 ns of simulation time. The results of this study provide insights how naproxen can specifically interact with the conserved RNA binding module of the nucleocapsid of SARS-CoV-2 that would inhibit the packaging of viral genome into capsid and virus assembly. Therefore we recommend evaluating the antiviral effects of naproxen against SARS-CoV-2 in *in vitro* studies and clinical trials.

Introduction

Coronaviruses, the causative agents of many pathological conditions in humans and animals are large single-stranded RNA viruses belonging to Coronaviridae. They are divided into 4 genera Alphacoronavirus, Betacoronavirus, Gammacoronavirus, and Deltacoronavirus[1]The genus Betacoronavirus contains some the most important respiratory viruses such as Severe acute respiratory syndrome-related coronavirus (SARS-CoV), Middle East respiratory syndrome- related coronavirus (MERS-CoV) and the newly identified one severe acute respiratory syndrome coronavirus 2 (SARS-CoV–2)[2]. SARS-CoV–2 was identified as the cause of a cluster of pneumonia cases in Wuhan, a city in the Hubei Province of China, at the end of 2019 [3] Since the first reports of cases from China, the number of infected diseases has been rising daily in this country and other countries [4]. The origin of SARS-CoV–2 was in enzootic bat viruses and then transmitted from presymptomatic or asymptomatic infected cases [5]. SARS-CoV–2 is closely related to SARS-CoV containing a 30kb genome organized into several ORFs necessary for viral infection and replication in the host cells. About 21 kb of the genome encodes for two large polyproteins pp1a and pp1ab that are processed into several nonstructural proteins of the virus by viral protease. SARS COV–2 also encodes for 4 structural proteins namely the spike (S), membrane (M), envelope (E), and nucleocapsid (N) proteins. The first three proteins are essential parts of viral capsid and envelope while the N protein takes part in the packaging of the genome into viral particle[6,7].

Crystallography studies of SARS-CoV and SARS CoV–2 nucleocapsids showed that the protein has two distinct domains at each terminus separated by intrinsically disorderedcentral Ser/Arg (SR)-rich linker. The N and C terminal domains are responsible for viral genome binding and nucleocapsid

dimerization/oligomerization respectively. The N terminal domain contains a conserved RNA binding domain that not only takes parts in the formation of viral ribonucleoprotein (RNP) complex but also in regulating the viral replication and transcription by maintaining highly ordered RNA conformation[8,9]

The conserved N and C terminal domains of the nucleocapsid of the virus have been proposed as potential drug targeting sites for inhibition of viral replication and assembly[8]. Two strategies can be considered for this purpose. First, structure-based drug design screening and synthesis for these domains that are time-consuming and expensive with a high rate of failure and potential unpredicted adverse effect on the human body. Second, repurposing commonly used drugs that are available in the market with known safety and adverse effect.

The incubation period for COVID–19 is thought to be within 14 days after exposure, with most cases present symptoms approximately five days following exposure [10]. Infections with SARS COV–2 are not severe in many cases, although most patients have had a critical illness [11–16]. Pneumonia is a serious manifestation of infection, characterized primarily by fever, cough, and dyspnea. Additionally, gastrointestinal symptoms such as nausea and diarrhea have been reported in some cases as an uncommon manifestation [12–14]. Management of patients with suspected or documented COVID–19 has two sections include appropriate infection controland supportive care [17]. There are no specific antiviral therapies for COVID–19 and there are many efforts for drug repurposing in all of the worlds [18,19]. For example, lopinavir-ritonavir combination therapy, as protease inhibitor which is used for the treatment of HIV infection, has antiviral activity against the SARS-CoV in vitro [20] and MERS-CoV in animal studies [21] and it could be used for treatment of COVID–19 in some patients [22,23]. Also, a randomized clinical trial in China is performing to evaluate the efficacy and safety of remdesivir as a nucleotide analogue in COVID–19 [17] due to its activity against SARS and MERS-CoVin both in vitro and animal studies [24,25].

Naproxen is a non-selective NSAIDs that inhibit the activity of both COX isoenzyme. NSAIDs is among the most widely used therapeutics with antipyretic and analgesic effect and they are choice treatment in various inflammatory diseases such as arthritis, rheumatism as well as relieving the pain of everyday life [26] Previous study shows that Naproxen had effective in influenza A and B as an antiviral activity in animal and clinical study [27–29]. It has been shown that naproxen interacts directly with the essential amino acids for viral RNA binding in the N terminal domain of the wild-type influenza A nucleoprotein, therefore, prevents the formation viral ribonucleoprotein (RNP) complex and subsequent virus production[29,30].

As most COVID19 patients complaints for having fever and myalgia [13,14,31] and presence of well-documented evidence for the specific interaction of naproxen with RNA binding domain of viral nucleoproteins [29,30], the aim of this study was to in silico evaluation of the antiviral effect of naproxen on SARS COV–2 and further recommendation of it as both antiviral and anti- inflammatorydrug in clinical trials.

Methods

Homology modeling

The full-length protein sequence of severe acute respiratory syndrome coronavirus 2's nucleocapsid (NP) was retrieved from NCBI Protein Database, accession number QIC53221. Since there is no complete template for the whole sequence (419 amino acids) and also the important functional parts of the protein located at its N (RNA binding domain) and C terminal domains(Dimerization domain) (Fig 1), two separate homology models were created.

Initially, the domains indicated in fig 1 were extracted and searched against the PDB database using BLAST-P to find an optimal template for each one.PDB ID 1ssk which is belonged to the Nterminal RNA-binding domain of the SARS CoVnucleocapsid protein [32]was selected as a template for the Nterminal domain (% Identity 93%). Similarly, Crystal structure of the SARS coronavirus nucleocapsid protein dimerization domain (PDB ID 2GIB) [33] at 1.75 Å resolution was used as the template for the Cterminal domain (% Identity 93%). Thereafter, the sequences and templates were aligned. The initial 30 models were created for each sequence and were sorted according to the GB/VI model. Since there is a very high similarity between the sequences and the templates there was no concern about the protein's loops reconstruction. The top model was refined to the highest level by energy minimization until the root mean square gradient falls below 0.001. Finally, the quality of the models was evaluated by the Ramachandran plot and SAVE Server. All of the modeling steps were conducted on the Molecular Operating Environment (MOE) 2019.01.02.In addition to the protein targets, the 3D model of the conserved stem-loop of the SARS COV–2 RNA packaging signal (Fig 2) was also predicted by the DNA/ RNA modeling module of Molsoft ICM-Pro 3.8.7c. This signal is critical for the NP to correctly recognize the viral genomic RNA and assemble it into the capsid.

Protein—Ligand Docking

To analyze the exact binding pose and calculate the approximation of the binding free energy between Naproxen with both domains of the NP protein, molecular docking was accomplished by molsoft ICM-Pro 3.8.7c. Initially, the modeled structures were prepared by adjusting hydrogen atoms, fixing the partial charges of the residues, etc. The ligand (Naproxen) was also retrieved from PubChem and converted to the 3D format. Subsequently, the binding pockets the both models were predicated and inspected visually. Thereafter, the docking grid was generated around the selected pocket. Finally, the fully flexible ligand was docked in the grid guided pocket of the semi-flexible N and Cterminal domains using a well-tested scoring function which has equipped with flexible ring sampling on the fly for better ligand fitting. The best binding pose was selected according to the docking score and visual inspections of the interacted residues. This pose was used in molecular dynamics simulation.Additionally, the most commonly prescribed NSAID for the alleviation of the SARS COV–2 induced lung inflammation,

ibuprofen, was docked in the same pocket of both proteins as an irrelevant compound for comparison purposes.

Protein—Protein Docking

To elucidate the possible interfering effect of naproxen binding on the RNA binding activity of N protein and also dimerization of C terminal domain, two independent protein—protein docking studies were performed using Global FFT Dock of Molsoft ICM-Pro 3.8.7c. In the 1st study, the conserved stem-loop of RNA packaging signal that was modeled earlier was docked at the empty RNA binding interface of the Nterminal domain. The top-scored pose was selected based on the interaction energy. The 2nd study was performed similarly. However, the N protein with naproxen bonded at its RNA binding pocket was used as the receptor. Any interference of reproducing the 1st study pose was investigated. A similar procedure with some modification was done for the Cterminal domain. The docking pocket for the Cterminal domain is the dimerization interface.

MM-GBSA Scoring

To estimate the correct free energy of binding between naproxen and its targets, the molecular mechanics energies approach combined with the generalized Born and surface area (MM-GBSA) was applied as a comprehensive modular nature approach for binding free energy calculation. To calculate this value, the MM-GBSA module of Schrodinger suite 2019–2 was used under OPLS3e forcefield in VSGB 2.0 solvation model. A 5 Å full flexibility of the receptor around the ligand with minimizing the sampling method was taken into account when the calculations were conducted.

Molecular Dynamics (MD) Simulation

The realistic interaction of naproxen with both proteins and also its effect on the protein structure was determined by 100 ns MD simulation in an explicit water model. For this purpose, the final modeled structures which were already docked with naproxen were dissolved in a layer of TIP3 water molecule with 10 Å distance from the edge of the protein. The systems were neutralized by adding 50mM counterions (NaCl). For simulating the biological condition, the MD was performed in NAMD 2.13 molecular dynamics engine (GPU accelerated version) under constant pressure and temperature under the NPT ensemble. Amber14-EHT forcefield was used for calculating the interaction potentials throughout the simulation. After preparing the systems, the MD was initiated according to the following protocol. Initially, the system was relaxed by 1 ns minimization step. Thereafter it was heated up to 310 K for 5 ns to bring the system out of local minima. The protocol was followed by 10 ns equilibration at the target temperature. Finally, the production step was executed for 100 ns with 2 fs timestep to solve the equation of motion. All light bonds length was constrained with the SHAKE algorithm. The system was sampled every 2 ps and the snapshot was analyzed for RMSD, RMSF, and interaction energy changes.

Results

Computational model of N and C Terminal Domains

The atomic-resolution modelsof both N and C terminal domains of SARS COV–2 were shown in Fig 3 in ribbon representation with their transparent electrostatic surface (Blue and Red are positive and negative residues respectively). As already described, the quality of the models was evaluated by both the Ramachandran plot (inset of Fig 3) and also SAVE server. The Ramachandran plots show there is no more than 0.5% of the residues were in the not allowable area which is more than the acceptable threshold (5%). The results of the SAVE server were also confirmatory. For N and C domains, 98.54% and 80.41% of the residues haveaveraged 3D–1D score ≥ 0.2 respectively. The N terminal domain is mainly β content. However, the C portion is α/β. The RMSD values between both protein and their templates are less than 0.2 Å. According to these results, the modeled structures meet the criteria for a good model.Besides, both proteins contain an exposed pocket (dashed box) surrounded by some charged residues. The key residues of the N terminal domain's pocket include R88 and R92 which have a critical role in the RNA binding function. However, the dimerization interface contains many residues although some of them such as F34, R37, and F46 are so important [33]. Besides the NP domain structures, a 27-nucleotide segment of the viral RNA packaging signal was also comparatively modeled and used for the docking step. The predicted model was demonstrated in Fig 4.

Protein- proteindocking

For elucidation of the hotspot of the modeled structures for the normal interaction with their substrates, the protein—protein docking was accomplished for both of them. The result of the N terminal domain docked to the RNA packaging signal was shown in Fig 5. Since the docking algorithm was induced flexibility in the RNA molecule, its structure undergoes some conformation changes compared to its initial state. As is clear, the best-docked pose indicates the RNA was exactly bound to the positively charged pocket (dock score –7.26 Kcal/mol) which was described in Fig 3. The residues involved in the binding process were also indicated in Fig 5b. Notably, two key residues, R88 and R92, were also present in the interaction interface. These residues coordinate the RNA molecule in the pocket through electrostatic interactions with the negatively charged backbone phosphate atoms. There are also two other important residues (Y109 and Y111) which boost the binding of the RNA molecule via pi-pi stacking interactions.

Similarly, the dimerization interface of the C terminal domain structure was also elucidated by superimposition guided manual protein- protein docking of the modeled structure to itself. The result was shown in Fig 6. As already described before and can be seen in this figure, this area includes many residues. Some of them may have a little more important role in binding such as F34, R37, and F46. However, the dimerization process requires almost equal participation from all residues.

Ligand Docking

The predicted top docking conformation of naproxen with the N and C terminal domains structures are shown in Fig 7 and 8. For the N terminal domain, the top-scored pose of the drug was accurately docked to the predicted active pocket of the protein that has been shown in Fig 3 (docking score –21.3 Kcal/mol). The ligand was stabilized inside the pocket through many interactions including but not limited to two salt bridges with both key Arginine residues (R88 and R92), a pi-anion with Y109, two pi-amid interactions with A50 and Y111 and two hydrogen bonds with backbones of G47 and T49. Among these interactions, the first two salt bridges are crucial for the proper binding of the RNA packaging signal [32]. Therefore, if a compound can mask these residues strongly, it may prevent the assembly of the virus by hindering the RNA packaging process. Moreover, the protein docking investigation was revealed when naproxen is bound to the described pocket, the RNA packaging signal cannot attach to this site which is a promising condition. When the top docked pose of the naproxen is compared with ibuprofen as anirrelevant drug (docking score –17.64 Kcal/mol), it can be seen that the binding strength of naproxen is greater. Ibuprofen binding site is similar to naproxen. It has many interactions with the pocket's residues which most of them are various types of pi stacking interactions (Fig 7c). It also had an H-bond with S51 which is absent for the naproxen interaction. However, it is missed a salt bridge interaction with one of the key arginine residues (R88). This may be the main reason for the lower binding affinity of this drug to the N terminal domain compared to naproxen.

The highest scored pose of binding between Cterminal domain protein and naproxen is demonstrated in fig 8. The affinity of naproxen to this domain is lower than the N terminal domain structure (docking score –16.3 for Cterminal domain vs. –21.3 for the N). It should be noted, although the dimerization interface includes a very wide area of the protein (fig 6b), only a little portion of it (the current binding pocket) has a druggabilitypotential. The binding region is mostly hydrophobic and, in this regard, the drug bound mainly through hydrophobic forces such as several pi-stacking interactions with V30, F34, F46, W61, I64. Besides, there is also a salt bridge to R37. By the way, the protein docking study is shown even when naproxen occupied its site in the Cterminal domain, the dimerization process did not hinder (fig 9). This could be due to the already described fact that the dimerization interface is very wide and go through among many residues and the naproxen binding occupies only a very small portion of it. Therefore, to the best of our knowledge and according to this result, it seems the naproxen is not an ideal intervention for inhibiting the NP dimerization. It is noteworthy that ibuprofen had a considerably better docking score than naproxen for this domain. However, the MM-GBSA evaluation did not confirm its superiority to naproxen (table 1).

Table 1. Summary of the MM-GBSA free energy of interaction

No.	Complex	Docking Score (kcal/mol)	MM-GBSA $\Delta G_{Binding}$ (kcal/mol)
1	Naproxen - N Domain	-21.3	-39.6
2	Naproxen - C Domain	-16.3	-38.4
3	Ibuprofen - N Domain	-17.6	-37.8
4	Ibuprofen - C Domain	-22.1	-35.9

Binding Free Energy Prediction

Since the MM-GBSA calculation is more accurate than any other scoring functions of molecular docking, the binding affinity of naproxen with the docked structures was reevaluated by this method again for double reassurance of the previous findings. The result is completely in accordance with the docking calculation and rank the naproxen binding capability to the N terminal domain at the top (Table 1) even though they used different forcefields. In conclusion, the reliability of the docking results was indicated.

Molecular Dynamics Simulation

To confirm the results that have been obtained from the molecular dockings and thermodynamic investigations, two rounds of MD simulations were performed on the top docked pose of both N and C terminal domains. Before analyzing the primary results, the stability of parameters of the systems was checked by plotting temperature and energy of the system during the equilibration step which revealed the systems were reached to a steady-state from (fluctuation of both parameters was less than 5% standard error during this step). The primary results of the simulation are shown in Fig 10. The RMSD plot for “Naproxen - N terminal Domain” showing the backbone of the structure deviated less than 7 Å during the whole 100 ns of the production step (fig 10a). Analysis of this plot indicates the trajectory reached to almost a steady state after 40 ns (variation of the RMSD is less than ±1Å). Twenty snapshots were taken from the system every 5 ns and visually inspected for the residues that are engaged in the interactions. In all of the samples, both key arginine residues (R88 and 92) have fully interacted with naproxen through electrostatic forces. In addition, analyzing the trajectory for h-bond formation shown, there is also at least one strong h-bond (acceptor-donor distance <3 Å) with naproxen throughout the simulation (e-value <0.05) (Fig 11a). This is a very promising finding, since the hydrogen bonding is crucial for stabilizing the ligand inside the receptor pocket.

The interaction energy was also completely in accordance with the other results especially the MM-GBSA, docking, and number of H-bond. It starts at –190.9 kcal/mol for the first frame and continues fairly steady to the end of the simulation with an average value of –184.4 Kcal/mol for all 50.000 frames. Fluctuation for each residue of this domain was demonstrated in the RMSF plot (Fig 10b). The average value for all of the residues is almost 4 Å with a lower and upper limit between 2.2 Å and 7.4 Å. These values indicate a medium fluctuation in the whole protein. The results also have shown that the key arginine residues reside in relatively low fluctuating region which is an indication of their important roles. Moreover, almost all regions that had a higher RMSF value have belonged to the loop structures.

All the above parameters were also investigated for the C terminal domain. As demonstrated in fig 10c and d, this domain had relatively higher values for the RMSD and RMSF plots. For example, although the

system correctly heated and equilibrated, however, the RMSD plot did not reach a perfect steady-state (the values gradually increased) until 80 ns. Likewise, the RMSF values for this domain approximately 2 Å higher than the N terminal domain (of course these are two different independent domains and it is not correct to compare them with each other). This is completely an expectable finding because of the nature of this domain which is designed for the dimerization, a process that requires higher flexibility not even in the contacting interface but also in the whole domain. The average RMSD value for this domain is about 5.81Å that is about 0.7 Å higher than the N terminal domain.

The interaction strength of naproxen with this domain is considerably lower than to the N terminal domain which was already specified by the MM-GBSA evaluation and also docking study. The interaction energy is started from −107.8 Kcal/mol and gradually decreased to lower than −250 Kcal/mol by 30 ns. However, it suddenly increased to more than −20 Kcal/mol by 35 ns. After this point, the interaction energy gradually become stronger until the end of simulation which reached −73 Kcal/mol with an average of −96.5 Kcal/mol for the whole period of simulation. This is about half the strength of naproxen interaction energywith the N terminal domain. Superimposing the number of H-bond on the interaction energy plot (Fig 11b) was revealed the sharp decrease in the interaction energy is probably due to the loose H-bonds at that time. Similar to the N terminal domain, 20 snapshots were taken from the system and visually inspected for he existed interactions. As expected, there is no stable pattern of interactions between snapshots.

Discussion

In this study, we showed comparative interaction of naproxen to the N terminal RNA- binding domain and C terminal dimerization/oligomerization domain of the nucleocapsid protein of SARS COV−2. We showed several key residues of the N terminal domain coordinate with naproxen that would compete for RNA binding with nucleocapsid. We also stimulated the binding dynamics of naproxen to N and C terminal domains during 100 ns of using molecular dynamics.

Nucleocapsid is one of the structural proteins of SARS COV−2 that is important for many functions including viral ribonucleoprotein (RNP) complex, regulation of replication or transcription. Crystallographic studies of the SARS-CoV N terminal domain revealed that the domain is folded mostly with antiparallel β-sheets core with a positively charged protruding hairpin, similarly, the same folding pattern has been seen for modeled and crystal structure of SARS-CoV−2 nucleocapsid [9]. Although the overall structure N terminal domains are the same among many betacoronavirus, the surface charge distribution pattern is markedly different [8] indicating unique RNA binding module for SARS COV−2. The C terminal domain of nucleocapsid also folds into a conserved structural shape resembling the letter C in the monomeric form among coronaviruses. As it has been modeled in this study C terminal domain folds into extended conformation with the dimerization surface at the center of the domain. The amino acids at the dimerization surface have been described for SARS-CoV which are mainly involved in hydrophilic and hydrophobic interactions[33]. Truncated nucleocapsid protein of SARS-CoV missing amino 285–422 inhibited the dimerization of nucleocapsid and virion assembly [34]

The molecular dynamics simulation that was done here, confirmed the data that were obtained by molecular docking and MM-GBSA evaluation and showed naproxen strongly interacted with the RNA binding pocket of the N terminal domain structure. By comparing with empty structure, it is clear that its flexibility did not affect significantly when naproxen bound (data not shown). It also should be noted that an intrinsic property of NP is its flexibility[35]. Our analysis following the other studies showed the two key arginine residues (R88 and R92) are bonded to naproxen in the whole simulation time. These residues are very important for the native RNA binding process and also present in the nucleocapsid of other viruses such as influenza[30,32]. In silicomutagenesis of these residues, the affinity of naproxen to the binding site drastically decreased. In addition to the electrostatic interactions, a network of H-bond between the ligand, protein and surrounding water molecules contributes to the stabilizing of the naproxenN terminal domain complex. Figure x11 shows this effect clearly. In this figure you can, the interaction energy completely obeys from the H-bond count between naproxen and the structures (this also was seen for the C terminal domain). For the N terminal domain, these strong interactions mask the RNA binding groove and compete with the viral RNA binding which similar to other studies on the anti-viral effect of this drug[36].We also examine the binding potential of naproxen to the C terminal domain because this requires protein dimerization which is essential for its normal function. Fig 10c, d show the way that this domain behaves. It has more flexibility than the N terminal domain which is completely in accordance with other findings that pointed out the flexibility of the C-terminal of NP is reminiscent[37,38].Possibly the higher flexibility interferes with the strong binding of naproxen with the key residues at the dimerization interface. By the way, as described in the result, occupying this site by naproxen cannot hinder the dimerization process which was deduced from the protein docking study.

High-throughput virtual screening and repurposing of the existing drugs for targeting SARS COV–2 proteins are the two main strategies for the rapid development of new anti-SARS COV–2 drugs. Using target-based virtual ligand screening, 18 putative proteins encoded by SARS COV- 2 were screened against the ZINC drug database and a local database.the results of this study showed three potential targets including 3-chymotrypsin-like protease (3CLpro), Spike, RNA- dependent RNA polymerase (RdRp), and papain-like protease (PLpro) with several lead compounds. However, such compounds were not identified for the nucleocapsid [39]

After the recent global outbreak of SARS COV–2 full-genome sequencing and phylogenic analysis indicated that SARS COV–2 is a betacoronavirus and similar to severe acute respiratory syndrome (SARS) virus. The receptor-binding gene structure of SARS COV–2 is alike with SARS coronavirus, and there is the same receptor for cell entry in both [40]. Additionally, the determination of the detailed 3D-structures of key virus proteins, it is very efficient to apply computer-aided drug design techniques to quickly identify promising drug repurposing candidates for virus elimination [41]. So, the aim of this insilico study was to determine the antiviral effect of naproxen on SARS COV–2 and the results of the present study showed that naproxen had interaction with two types of arginine, ARG A 49 and ARG A 45, which play a major role in RNA binding in whole transcriptional processes. Naproxen binds to the nucleocapsid site and does not allow the virus to bind to the cells. Previously, Zheng et al show that the NP of influenza

B virus (BNP) has a higher binding affinity to naproxen than influenza A virus NP (ANP) and specifically, naproxen targets the NP at residues F209 (BNP) and Y148 (ANP) [27]. In another study,Lejal et al by in silico screening showed that naproxen combined antiviral and anti-inflammatory effects by targeting both NP and COX2 in influenza A virus [36].

The result of the present study about COVID–19 and other studies about influenza show that nucleocapsid has a main role in the life cycle of coronaviruses and it is a target for naproxen. Nucleoprotein acts as a single-stranded RNA binding protein that takes on a significant role in ribonucleoprotein particles (RNPs) transporting between the nucleus and cytoplasm and it is a structural protein of RNPs that is required for virus replication [42]. Docking studies show that several known drugs such as Carfilzomib, Eravacycline, Valrubicin, Lopinavir, and Elbasvir. Carfilzomib, Streptomycin, and formoterol have an inhibitory effect against SARS COV–2 [43,44]. These drugs in-comparison with Naproxen are expensive and additionally, Naproxen is a drug in controlling some symptoms of these patients, such as fever and myalgia, so, it seems that is preferred over other drugs. Therefore, due to the antiviral role of naproxen, it is recommended to use naproxen in patients infected with SARS COV–2 without drug contraindication to help control fever and virus clearance time.

Conclusion

The urgent demand for the development of new antiviral drugs for the treatment of COVID–19 patients has led us to repurpose a commonly used antipyretic and analgesic drug for specific treatment of SARS COV–2 infect patients. In this study using molecular docking and molecular dynamics analysis, we showed that naproxen interacts specifically with some key amino acids in the RNA binding pocket of the N terminal domain of SARS COV–2 nucleocapsid. The results of this study also indicate naproxen might compete with viral RNA for biding with nucleocapsid therefore inhibiting viral capsid assembly and viral particle formation. Based on promising results obtained in this study we suggest further in vitro experiments and clinical trials to use naproxen in the treatment of COVID–19 patients.

Declarations

Acknowledgments:

This research was supported by Mazandaran University of Medical Sciences (Grant no: 7274)

Author contributions:

R.V, R.A, F.R, designed and convinced the project.R.V., M.L. performed the bioinformatics analysis. R.V., R.A., M.L., M.S., F.R., A.H., M.A wroteand edited the manuscript.

Competing interests

The authors declare no competing interests.

References

1. Pan, F. *et al.* Time Course of Lung Changes On Chest CT During Recovery From 2019 Novel Coronavirus (COVID-19) Pneumonia. *Radiology*, 200370, doi:10.1148/radiol.2020200370 (2020).
2. Tarus, B. *et al.* Structure-based design of novel naproxen derivatives targeting monomeric nucleoprotein of Influenza A virus. *J Biomol Struct Dyn***33**, 1899-1912, doi:10.1080/07391102.2014.979230 (2015).
3. Dilly, S. *et al.* From Naproxen Repurposing to Naproxen Analogues and Their Antiviral Activity against Influenza A Virus. *J Med Chem***61**, 7202-7217, doi:10.1021/acs.jmedchem.8b00557 (2018).
4. Hung, I. F. N. *et al.* Efficacy of Clarithromycin-Naproxen-Oseltamivir Combination in the Treatment of Patients Hospitalized for Influenza A(H3N2) Infection: An Open-label Randomized, Controlled, Phase IIb/III Trial. *Chest***151**, 1069-1080, doi:10.1016/j.chest.2016.11.012 (2017).
5. Zheng, W. *et al.* Naproxen Exhibits Broad Anti-influenza Virus Activity in Mice by Impeding Viral Nucleoprotein Nuclear Export. *Cell reports***27**, 1875-1885.e1875, doi:10.1016/j.celrep.2019.04.053 (2019).
6. Zarghi, A. & Arfaei, S. Selective COX-2 Inhibitors: A Review of Their Structure-Activity Relationships. *Iranian journal of pharmaceutical research : IJPR***10**, 655-683 (2011).
7. Wang, M. *et al.* Remdesivir and chloroquine effectively inhibit the recently emerged novel coronavirus (2019-nCoV) in vitro. *Cell research***30**, 269-271, doi:10.1038/s41422-020-0282-0 (2020).
8. Sheahan, T. P. *et al.* Broad-spectrum antiviral GS-5734 inhibits both epidemic and zoonotic coronaviruses. *Science translational medicine***9**, doi:10.1126/scitranslmed.aal3653 (2017).
9. Wang, Z., Chen, X., Lu, Y., Chen, F. & Zhang, W. Clinical characteristics and therapeutic procedure for four cases with 2019 novel coronavirus pneumonia receiving combined Chinese and Western medicine treatment. *Bioscience trends*, doi:10.5582/bst.2020.01030 (2020).
10. Lim, J. *et al.* Case of the Index Patient Who Caused Tertiary Transmission of COVID-19 Infection in Korea: the Application of Lopinavir/Ritonavir for the Treatment of COVID-19 Infected Pneumonia Monitored by Quantitative RT-PCR. *Journal of Korean medical science***35**, e79, doi:10.3346/jkms.2020.35.e79 (2020).
11. Chan, J. F. *et al.* Treatment With Lopinavir/Ritonavir or Interferon-beta1b Improves Outcome of MERS-CoV Infection in a Nonhuman Primate Model of Common Marmoset. *The Journal of infectious diseases***212**, 1904-1913, doi:10.1093/infdis/jiv392 (2015).
12. Groneberg, D. A. *et al.* Treatment and vaccines for severe acute respiratory syndrome. *The Lancet. Infectious diseases***5**, 147-155, doi:10.1016/s1473-3099(05)01307-1 (2005).
13. Xu, J., Shi, P. Y., Li, H. & Zhou, J. Broad Spectrum Antiviral Agent Niclosamide and Its Therapeutic Potential. *ACS infectious diseases*, doi:10.1021/acsinfecdis.0c00052 (2020).
14. Yao, T. T., Qian, J. D., Zhu, W. Y., Wang, Y. & Wang, G. Q. A systematic review of lopinavir therapy for SARS coronavirus and MERS coronavirus-A possible reference for coronavirus disease-19 treatment option. *Journal of medical virology*, doi:10.1002/jmv.25729 (2020).

15. McIntosh, K. *Coronavirus disease 2019 (COVID-19)*, <14> (2020).
16. Wu, Z. & McGoogan, J. M. Characteristics of and Important Lessons From the Coronavirus Disease 2019 (COVID-19) Outbreak in China: Summary of a Report of 72314 Cases From the Chinese Center for Disease Control and Prevention. *Jama*, doi:10.1001/jama.2020.2648 (2020).
17. Yang, X. *et al.* Clinical course and outcomes of critically ill patients with SARS-CoV-2 pneumonia in Wuhan, China: a single-centered, retrospective, observational study. *The Lancet. Respiratory medicine*, doi:10.1016/s2213-2600(20)30079-5 (2020).
18. Wang, D. *et al.* Clinical Characteristics of 138 Hospitalized Patients With 2019 Novel Coronavirus-Infected Pneumonia in Wuhan, China. *Jama*, doi:10.1001/jama.2020.1585 (2020).
19. Chen, N. *et al.* Epidemiological and clinical characteristics of 99 cases of 2019 novel coronavirus pneumonia in Wuhan, China: a descriptive study. *Lancet (London, England)***395**, 507-513, doi:10.1016/s0140-6736(20)30211-7 (2020).
20. Huang, C. *et al.* Clinical features of patients infected with 2019 novel coronavirus in Wuhan, China. *Lancet (London, England)***395**, 497-506, doi:10.1016/s0140-6736(20)30183-5 (2020).
21. Chan, J. F. *et al.* A familial cluster of pneumonia associated with the 2019 novel coronavirus indicating person-to-person transmission: a study of a family cluster. *Lancet (London, England)***395**, 514-523, doi:10.1016/s0140-6736(20)30154-9 (2020).
22. Li, Q. *et al.* Early Transmission Dynamics in Wuhan, China, of Novel Coronavirus-Infected Pneumonia. *The New England journal of medicine*, doi:10.1056/NEJMoa2001316 (2020).
23. Saikatendu, K. S. *et al.* Ribonucleocapsid formation of severe acute respiratory syndrome coronavirus through molecular action of the N-terminal domain of N protein. *J Virol***81**, 3913- 3921, doi:10.1128/JVI.02236-06 (2007).
24. Kang, S. *et al.* Crystal structure of SARS-CoV-2 nucleocapsid protein RNA binding domain reveals potential unique drug targeting sites. *bioRxiv*, 2020.2003.2006.977876, doi:10.1101/2020.03.06.977876 (2020).
25. Cong, Y. *et al.* Nucleocapsid Protein Recruitment to Replication-Transcription Complexes Plays a Crucial Role in Coronaviral Life Cycle. *J Virol***94**, doi:10.1128/JVI.01925-19 (2020).
26. Wu, F. *et al.* A new coronavirus associated with human respiratory disease in China. *Nature***579**, 265-269, doi:10.1038/s41586-020-2008-3 (2020).
27. Morens, D. M., Daszak, P. & Taubenberger, J. K. Escaping Pandora's Box - Another Novel Coronavirus. *The New England journal of medicine*, doi:10.1056/NEJMp2002106 (2020).
28. Cao, Y. *et al.* Hospital Emergency Management Plan During the COVID-19 Epidemic. *Academic emergency medicine : official journal of the Society for Academic Emergency Medicine*, doi:10.1111/acem.13951 (2020).
29. Zhu, N. *et al.* A Novel Coronavirus from Patients with Pneumonia in China, 2019. *The New England journal of medicine***382**, 727-733, doi:10.1056/NEJMoa2001017 (2020).

30. Coronaviridae Study Group of the International Committee on Taxonomy of, V. The species Severe acute respiratory syndrome-related coronavirus: classifying 2019-nCoV and naming it SARS-CoV-2. *Nat Microbiol*, doi:10.1038/s41564-020-0695-z (2020).
31. Masters, P. S. The molecular biology of coronaviruses. *Adv Virus Res***66**, 193-292, doi:10.1016/S0065-3527(06)66005-3 (2006).
32. Huang, Q. *et al.* Structure of the N-terminal RNA-binding domain of the SARS CoV nucleocapsid protein. *Biochemistry***43**, 6059-6063, doi:10.1021/bi036155b (2004).
33. Yu, I. M., Oldham, M. L., Zhang, J. & Chen, J. Crystal structure of the severe acute respiratory syndrome (SARS) coronavirus nucleocapsid protein dimerization domain reveals evolutionary linkage between corona- and arteriviridae. *J Biol Chem***281**, 17134-17139, doi:10.1074/jbc.M602107200 (2006).
34. Yu, I. M. *et al.* Recombinant severe acute respiratory syndrome (SARS) coronavirus nucleocapsid protein forms a dimer through its C-terminal domain. *J Biol Chem***280**, 23280-23286, doi:10.1074/jbc.M501015200 (2005).
35. Tarus, B. *et al.* Molecular dynamics studies of the nucleoprotein of influenza A virus: role of the protein flexibility in RNA binding. *PLoS One***7**, e30038, doi:10.1371/journal.pone.0030038 (2012).
36. Lejal, N. *et al.* Structure-based discovery of the novel antiviral properties of naproxen against the nucleoprotein of influenza A virus. *Antimicrob Agents Chemother***57**, 2231-2242, doi:10.1128/AAC.02335-12 (2013).
37. Longhi, S. *et al.* The C-terminal domain of the measles virus nucleoprotein is intrinsically disordered and folds upon binding to the C-terminal moiety of the phosphoprotein. *J Biol Chem***278**, 18638-18648, doi:10.1074/jbc.M300518200 (2003).
38. Ruigrok, R. W., Crepin, T. & Kolakofsky, D. Nucleoproteins and nucleocapsids of negative-strand RNA viruses. *Curr Opin Microbiol***14**, 504-510, doi:10.1016/j.mib.2011.07.011 (2011).
39. Wu, C. *et al.* Analysis of therapeutic targets for SARS-CoV-2 and discovery of potential drugs by computational methods. *Acta Pharmaceutica Sinica B*, doi:https://doi.org/10.1016/j.apsb.2020.02.008 (2020).
40. Lu, R. *et al.* Genomic characterisation and epidemiology of 2019 novel coronavirus: implications for virus origins and receptor binding. *Lancet (London, England)***395**, 565-574, doi:10.1016/s0140-6736(20)30251-8 (2020).
41. Wang, J. Fast Identification of Possible Drug Treatment of Coronavirus Disease -19 (COVID-19) Through Computational Drug Repurposing Study. *ChemRxiv*, doi:10.26434/chemrxiv.11875446.
42. Tok, T. & Tatar, G. Structures and Functions of Coronavirus Proteins: Molecular Modeling of Viral Nucleoprotein. *Int J Virol Infect Dis***2**, 001 (2017).
43. Rimanshee, A., Amit, D., Vishal, P.&Mukesh, K. Potential inhibitors against papain-like protease of novel coronavirus (SARS-CoV-2) from FDA approved drugs. 2020.*ChemRxiv*, doi:26434/chemrxiv.11860011.v2 (2020).

44. Wang, J. Fast Identification of Possible Drug Treatment of Coronavirus Disease-19 (COVID-19) Through Computational Drug Repurposing Study. *ChemRxiv*, doi:10.26434/chemrxiv.11875446.v1 (2020).

Figures

Figure 1

A schematic representation of the most important functional domain of the Nucleocapsid Protein of COVID-19.

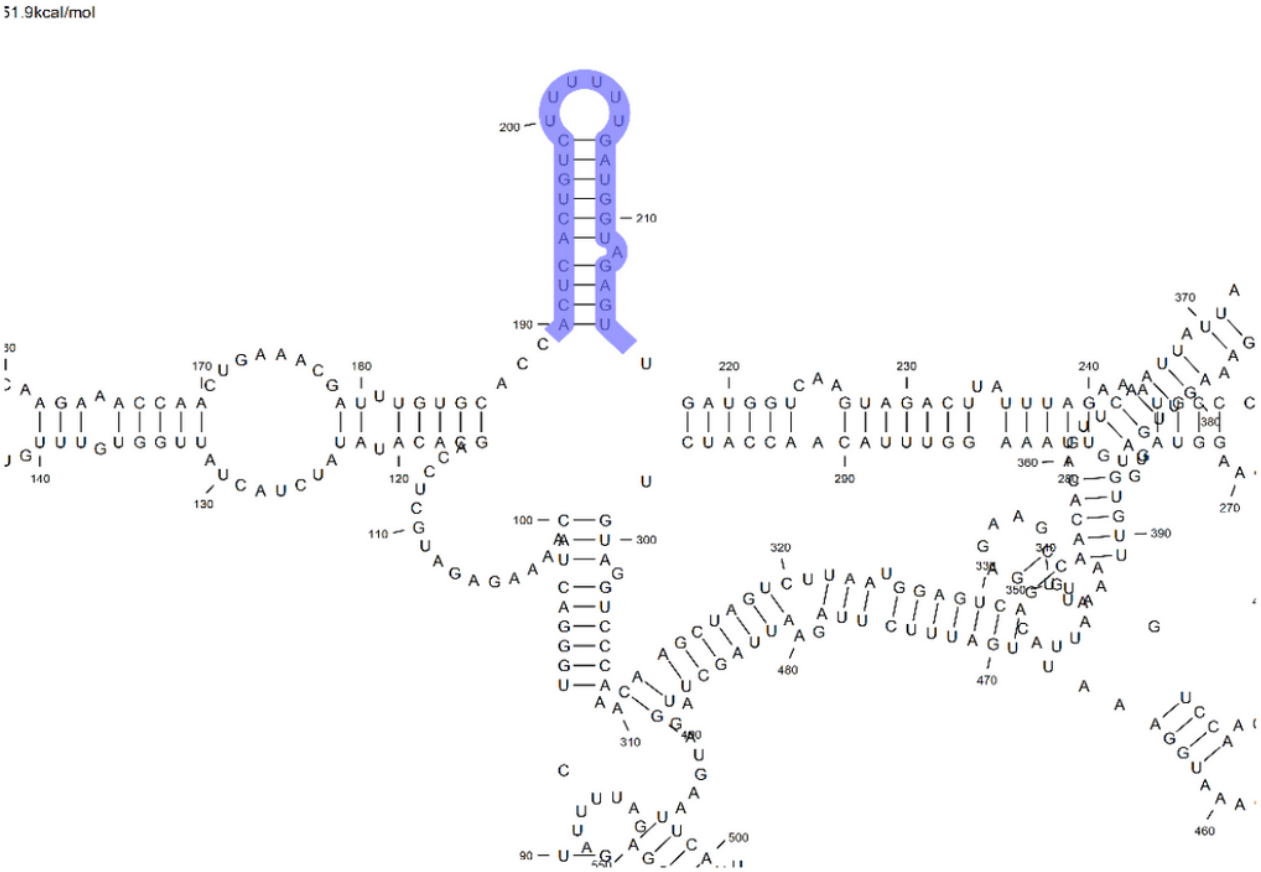

Figure 2

A schematic demonstration of the secondary structures of the RNA packaging signal of SARS-CoV-2. The blue highlighted region is the modeled segment which is required for the genuine binding and recognition.

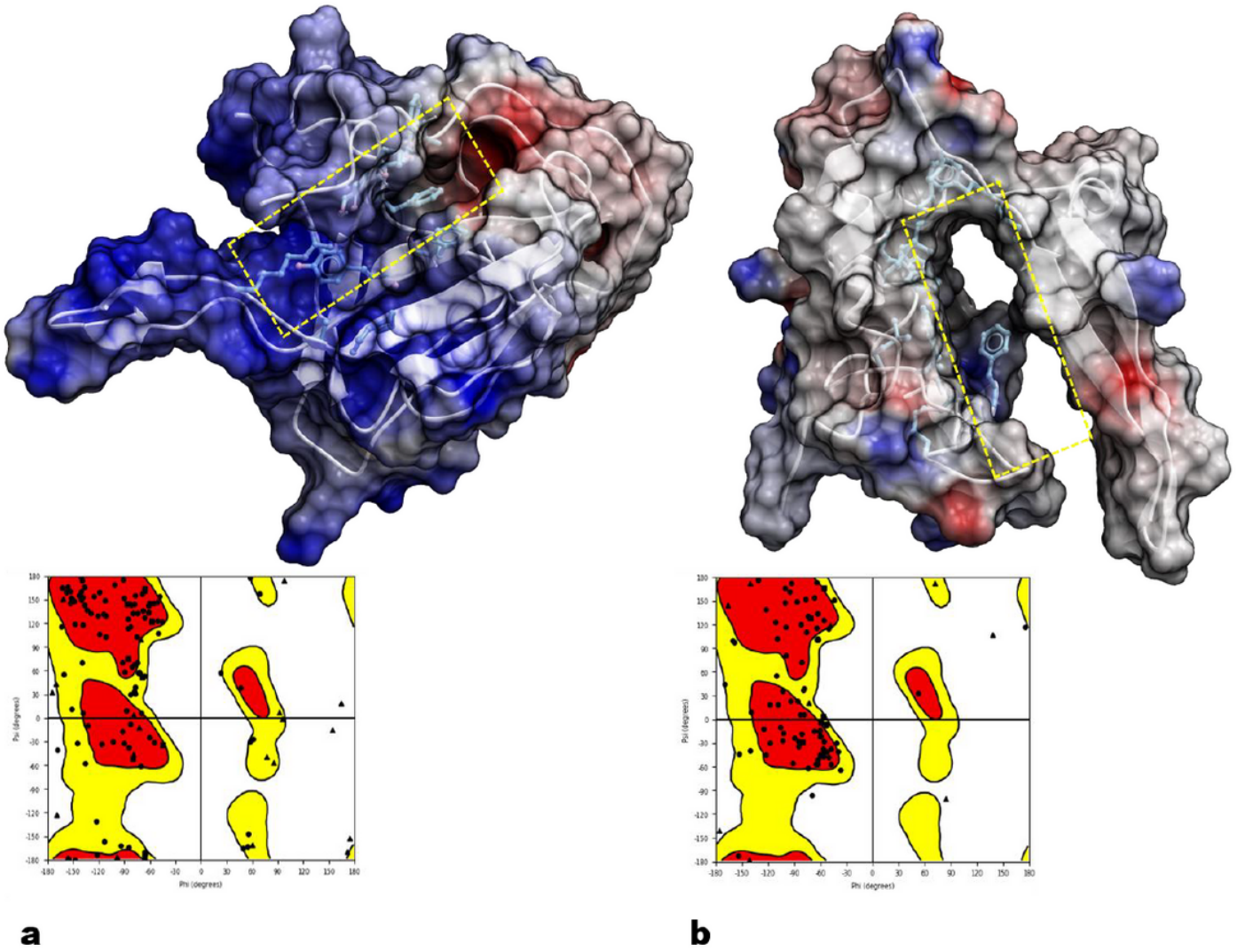

Figure 3

The atomic-resolution homology models of N terminal domain (a) and C terminal domain (b) of Severe acute respiratory syndrome coronavirus 2's nucleocapsid. The Ramachandran plot for structures was shown as an inset in the below of them (▲: Glycine, ■: Proline and ●: other residues). The location of the binding pocket/ dimerization domain was shown by the dashed yellow box for each structure.

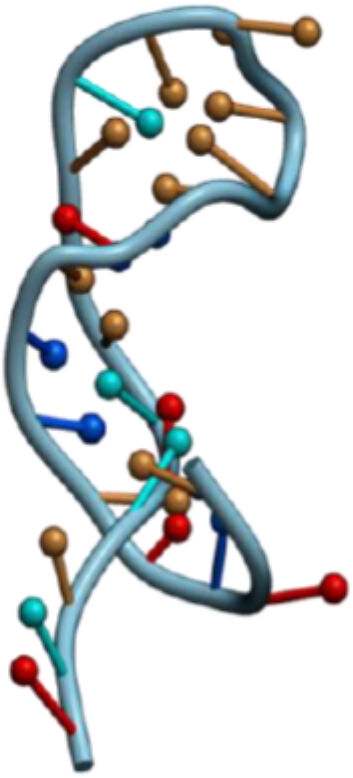

Figure 4

The homology model of the conserved stem-loop of the SARS-CoV-2RNA packaging signal.

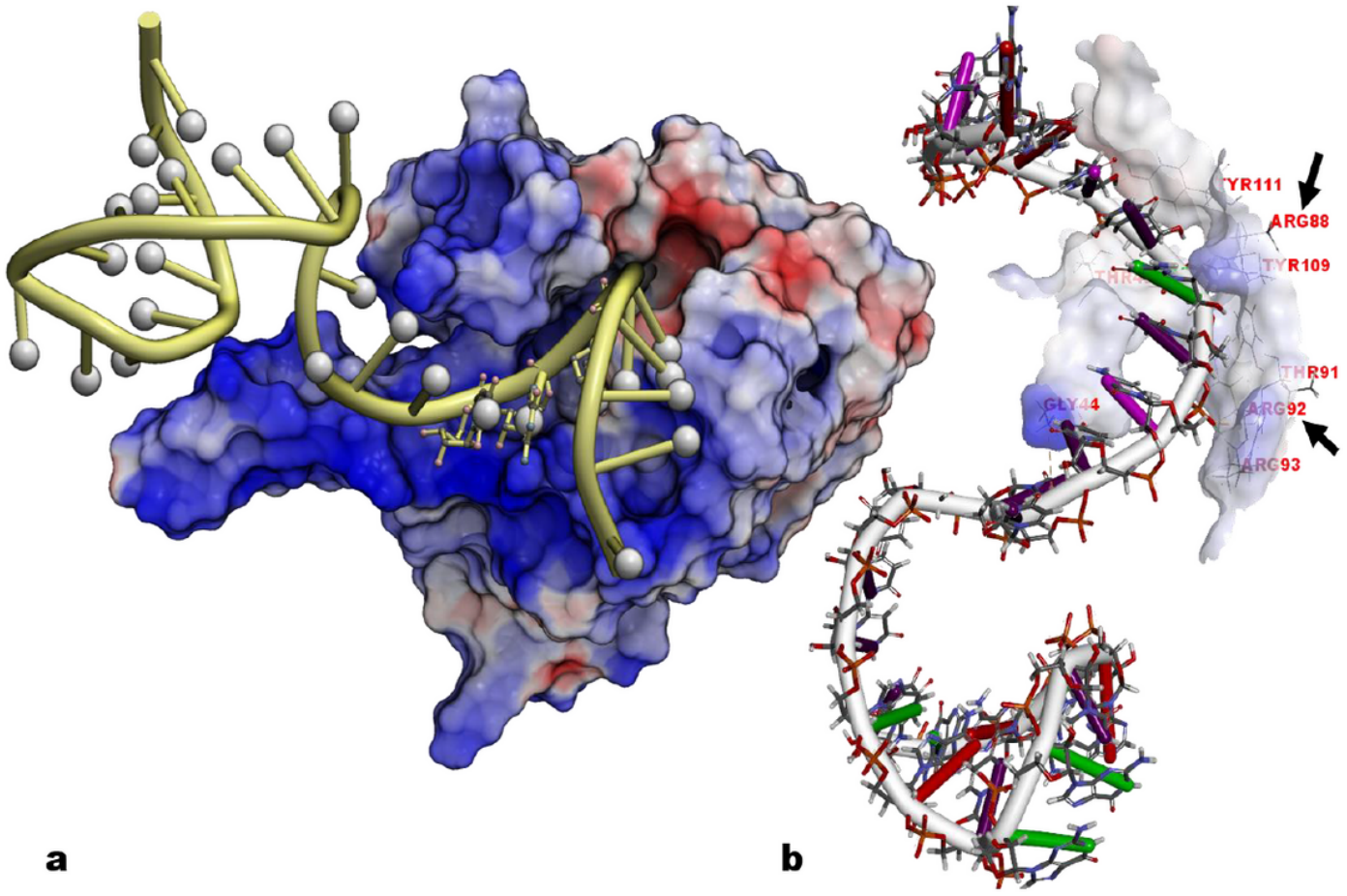

Figure 5

The best docking pose between N terminal domain structure (in an electrostatic surface representation| blue: positive residues, red: negative residues) and the conserved stem-loop of the SARS-CoV-2RNA packaging signal (a) and the residues involved in the binding process (b). The key arginine residues (R88 and R92) were indicated by black arrows.

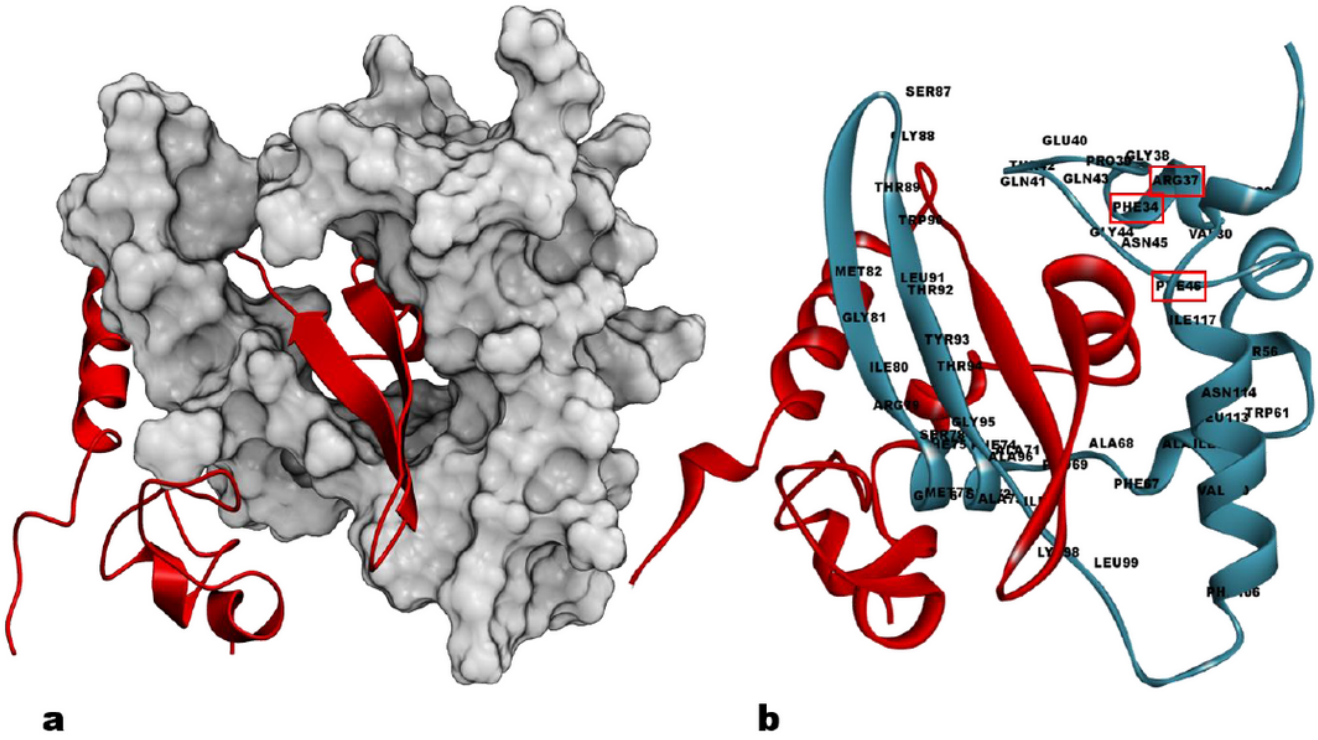

Figure 6

The homodimer homology model of the C terminal domain structure (a) with all of the participating residues at the dimerization interface (b). In part a, one of the monomers was shown in surface representation and another in ribbon style. In part b, the residues from only one of the chains had been shown and more important residues were indicated by the red box.

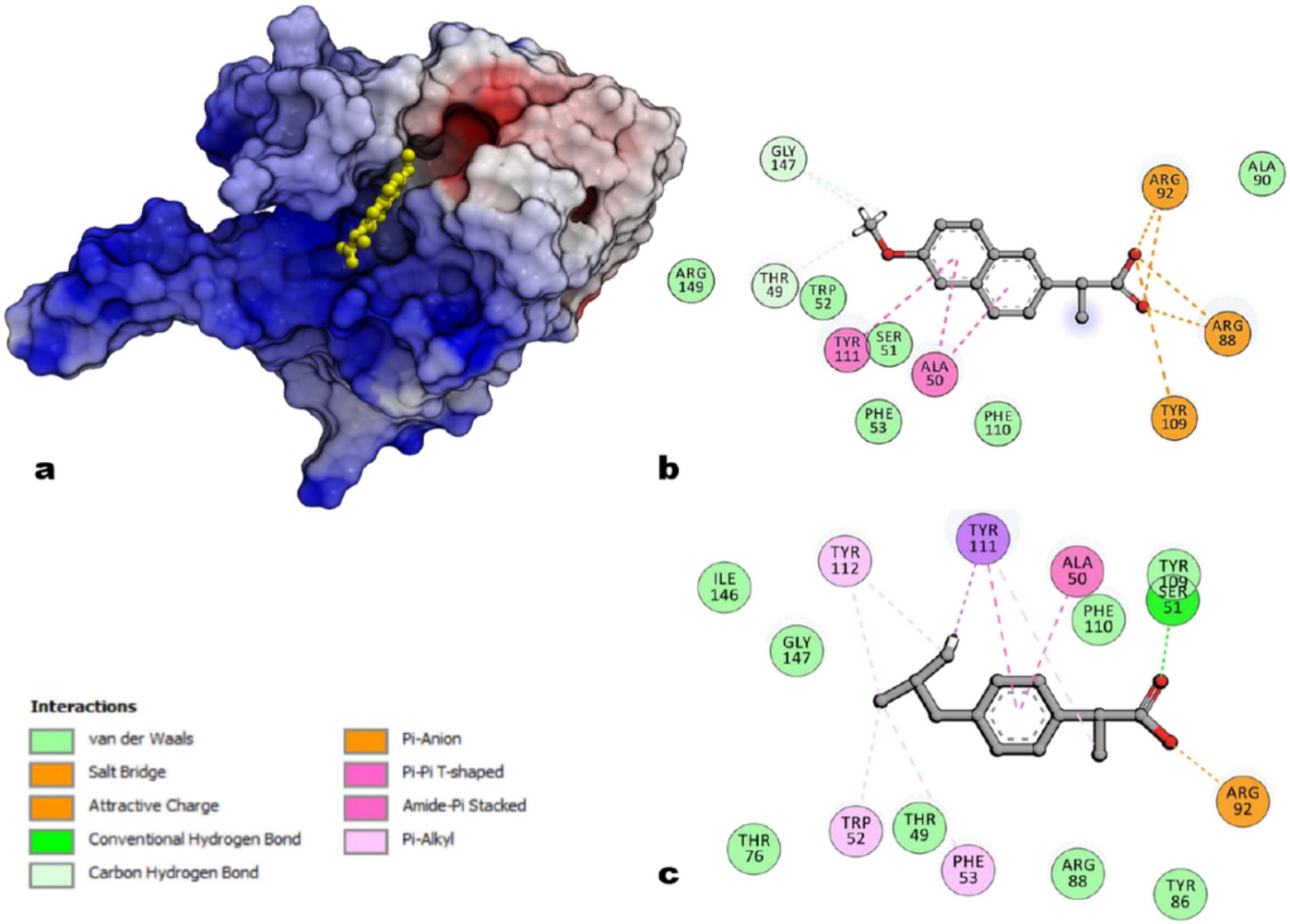

Figure 7

An electrostatic surface representation of the top docking pose between the N terminal domain structure of SARS-CoV-2NP protein and naproxen (a) and its 2D interaction diagram (b). The 2D interaction plot between ibuprofen and this domain was also demonstrated in part c. The interaction legend is shown in the lower left corner.

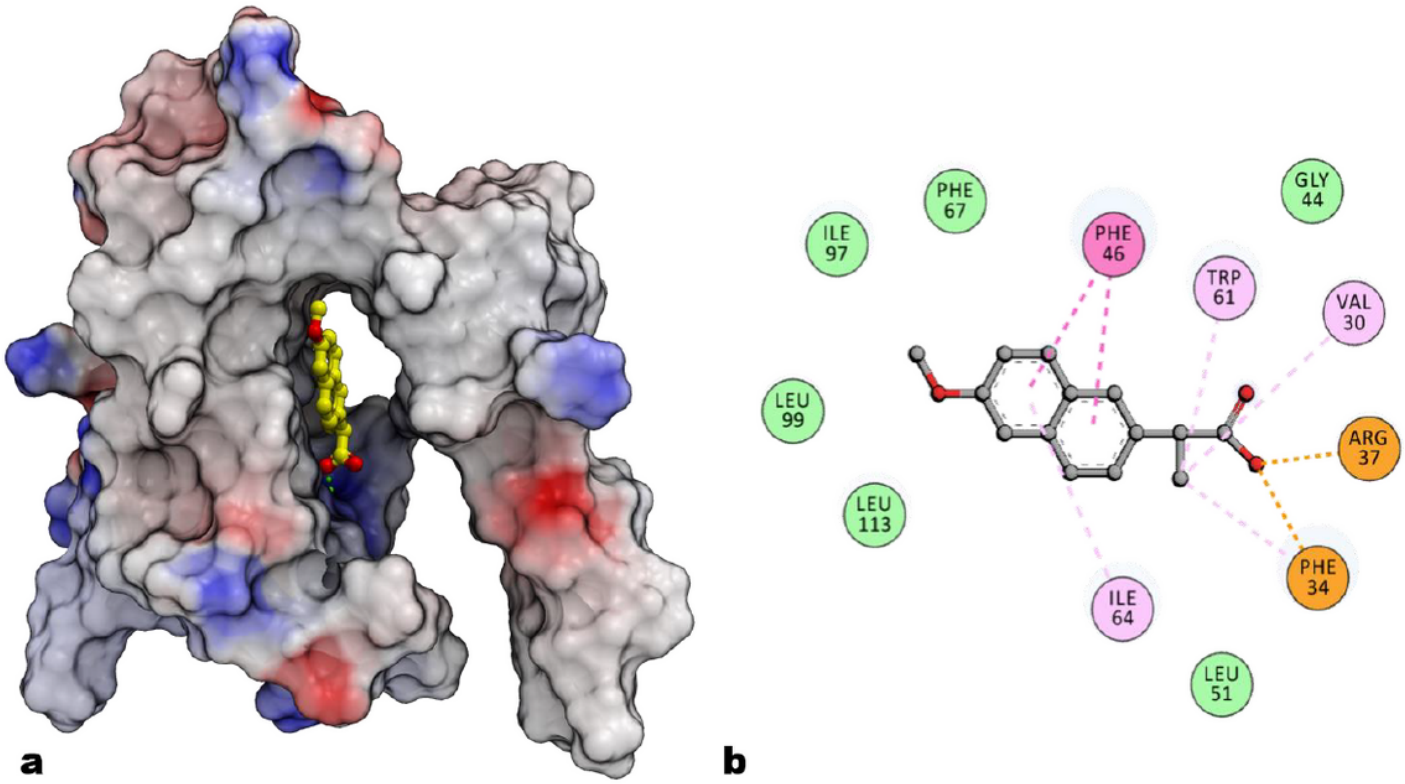

Figure 8

(a) The highest scored pose of docking between C terminal domain structure and naproxen. The protein was demonstrated in an electrostatic surface representation. The view angle is similar to fig 3b. (b) The 2D interacting diagram between naproxen and the C terminal domain structure. For more information please refer to the text. The legend of the interactions is similar to fig 7

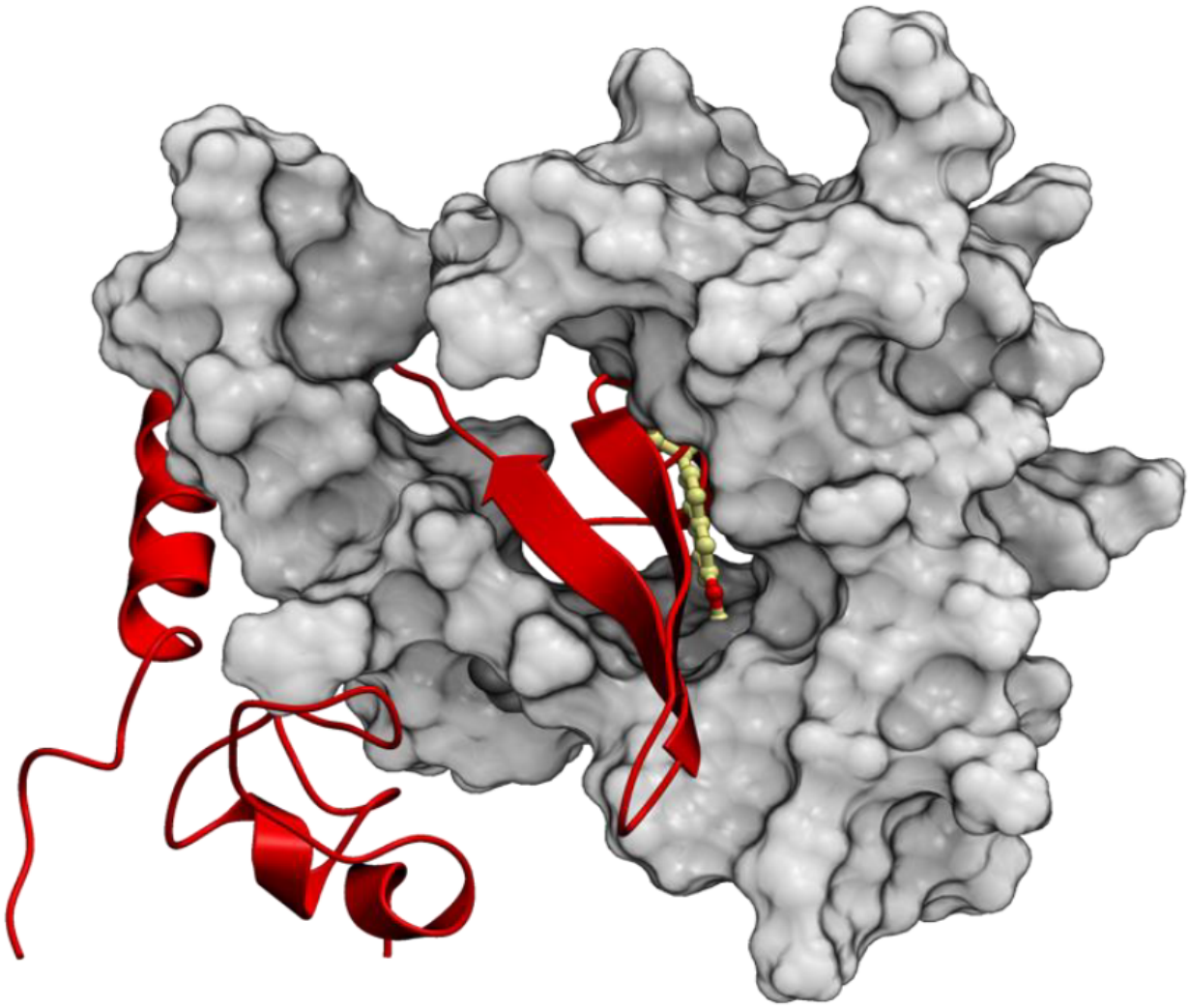

Figure 9

The C terminal domain was dimerized while naproxen bound to its pocket. This is suggested that the compound may fail from inhibiting the dimerization process which is vital for the correct NP function.

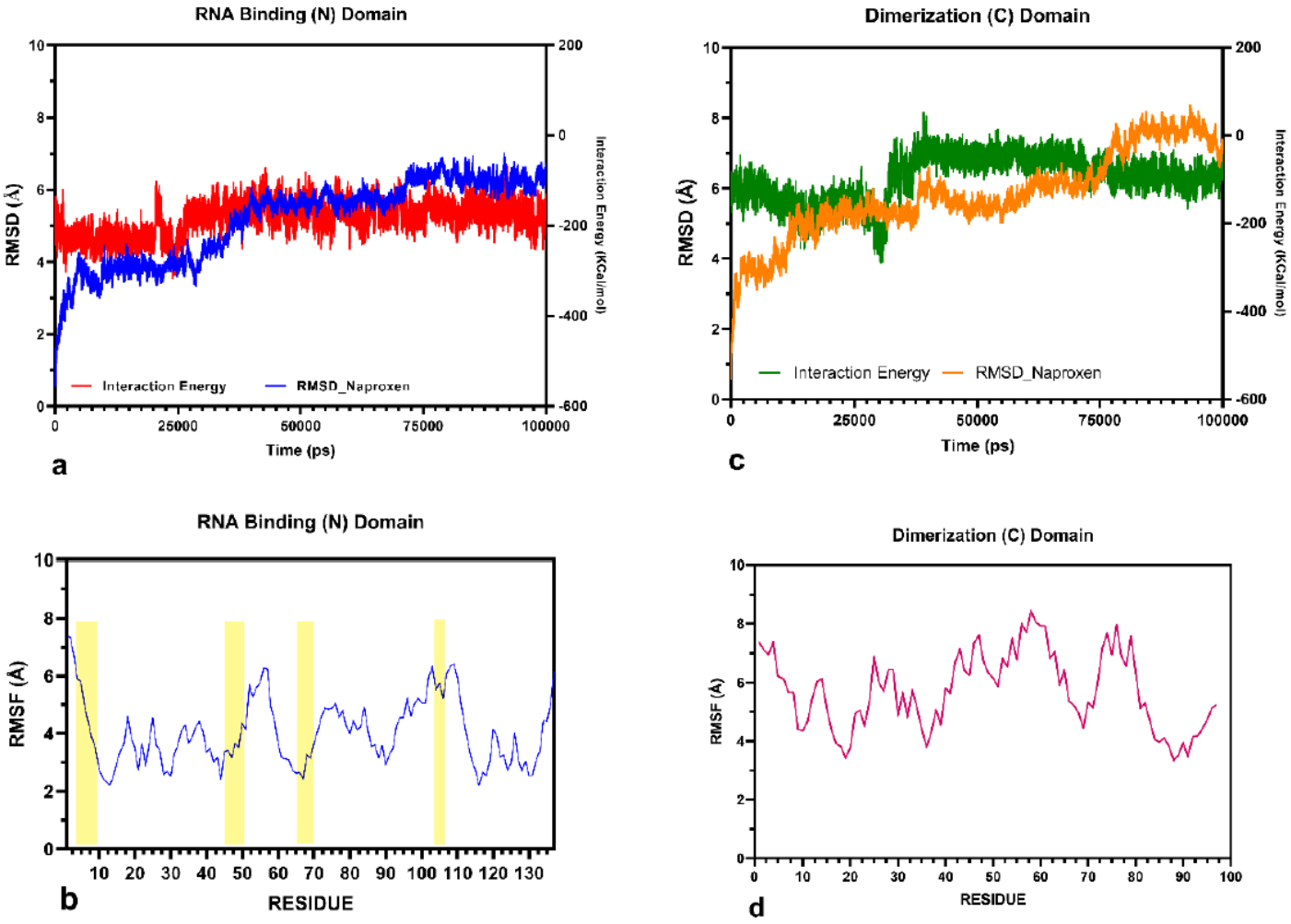

Figure 10

Backbone RMSD, whole residue RMSF and interaction energy plots of naproxen bound N (a, b) and C terminal domains (c, d). The RMSF plot of both proteins showed considerable fluctuation in the structures, although it is higher for the C terminal domain (d). The yellow highlights in (c) indicate the location of the residues in the binding pockets.

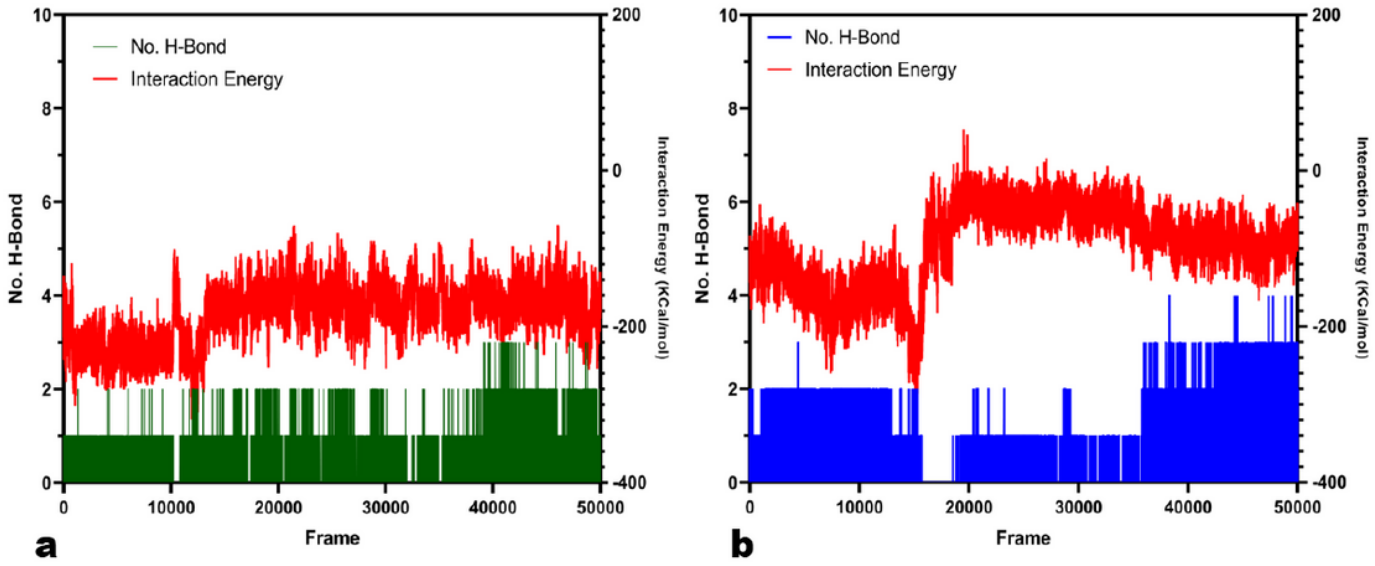

Figure 11

H-bond number plot between the N (a) and C (b) terminal domains and Naproxen superimposed on their interaction energy. The dependency of the interaction energy with the number of H-bonds can be seen clearly.